J Solid State Electrochem (2012) 16:1405–1414
DOI 10.1007/s10008-011-1519-0

ORIGINAL PAPER

Preparation of poly(vinylidene fluoride) nanocomposite membranes based on graft polymerization and sol–gel process for polymer electrolyte membrane fuel cells

Won Seok Chi · Rajkumar Patel · Hyungkwon Hwang · Yong Gun Shul · Jong Hak Kim

Received: 31 January 2011 / Revised: 30 July 2011 / Accepted: 1 August 2011 / Published online: 6 September 2011

Abstract Proton conducting nanocomposite membranes consisting of poly(vinylidene fluoride-*co*-chlorotrifluoroethylene)-graft-poly(styrene sulfonic acid), i.e., P(VDF-*co*-CTFE)-*g*-PSSA graft copolymer and sulfonated silica and were prepared using a sol–gel reaction and subsequent oxidation of a silica precursor, i.e., (3-mercaptopropyl) trimethoxysilane (MPTMS). The successful formation of amorphous phase nanocomposite membranes was confirmed via FT-IR and wide-angle X-ray scattering. All membranes were semi-transparent and mechanically strong, as characterized by a universal tensile machine. Transmission electron microscopy and small-angle X-ray scattering analysis revealed that silica 5–10 nm in size were homogeneously dispersed in the matrix at up to 5 wt.% of MPTMS. At higher concentrations, the silica grew to more than 50 nm in size, which disrupted the microphase-separated structure of the graft copolymer. As a result, both proton conductivity (0.12 S/cm at 25 °C) and single cell performance (1.0 W/cm^2 at 75 °C) were maximal at 5 wt.% MPTMS.

Keywords Graft copolymer · Nanocomposite · Polymer electrolyte membrane · Fuel cell · Proton conductivity

Introduction

Fuel cells have received considerable attention due to the direct conversion of chemical energy into electrical energy with high efficiency and low emission of pollutants [1–4]. Among the various types of fuel cells, polymer electrolyte membrane fuel cells (PEMFC) are new promising power sources for vehicles and portable devices. Membranes used in PEMFC applications are mostly based on perfluorinated polymers such as Nafion®. Although these membranes have demonstrated good electrochemical performance and long-term stability, their high cost and methanol crossover make them impractical for large-scale production. Therefore, the identification of alternative PEMFC materials is of pivotal importance [5–9].

Organic/inorganic nanocomposites are promising materials for many applications due to their extraordinary properties resulting from the synergism between the properties of the two different units. In particular, nanocomposite polymer electrolyte membranes produced via a sol–gel process have provided better mechanical stability and the necessary properties of proton conduction and water retention [10–15]. Nanocomposite membranes consisting of Nafion and silica have been prepared through the sol–gel reaction of tetraethoxysilane to form silica [16]. Recent studies have reported that the introduction of silica-based inorganic components derived from (3-mercaptopropyl) trimethoxysilane (MPTMS) can result in the formation of a homogeneous nanocomposite membrane with enhanced physicochemical stability and performance [17–19]. These MPTMS-based functional nanocomposite membranes possess high mechanical, thermal and chemical stabilities, low gas permeabilities, and high proton conductivities over wide temperature and humidity ranges.

In this study, poly(vinylidene fluoride-*co*-chlorotrifluoroethylene), P(VDF-*co*-CTFE), was grafted with poly(styrene sulfonic acid) via atom transfer radical polymerization (ATRP) to prepare a proton-conducting P(VDF-*co*-CTFE)-*g*-PSSA graft copolymer. The resultant graft copolymer was

W. S. Chi · R. Patel · H. Hwang · Y. G. Shul (✉) · J. H. Kim (✉)
Department of Chemical and Biomolecular Engineering,
Yonsei University,
262 Seongsanno, Seodaemun-gu,
Seoul 120-749, South Korea
e-mail: shulyg@yonsei.ac.kr
e-mail: jonghak@yonsei.ac.kr

combined with a silica precursor, MPTMS, via a sol–gel reaction and a subsequent oxidation process. The resulting nanocomposite membranes were characterized in detail using Fourier transform infrared spectroscopy (FT-IR), wide-angle X-ray scattering (WAXS), transmission electron microscopy (TEM), small-angle X-ray scattering (SAXS), universal tensile machine (UTM) testing, and thermogravimetric analysis (TGA). The proton conductivities of membranes and the single cell performance of the membrane electrode assembly (MEA) are also reported.

Experimental

Materials

P(VDF-*co*-CTFE) (PVDF SOLEF 31508/1001) was kindly provided by Solvay. 4-Styrene sulfonic acid (SSA) sodium salt hydrate, copper (I) chloride (CuCl), 1,1,4,7,10,10 hexamethyltriethylenetetramine (HMTETA), hydrogen peroxide, MPTMS, dimethyl sulfoxide (DMSO), and *N*-methyl-2-pyrrolidone (NMP) were purchased from Aldrich and were used as received without further purification.

Synthesis of graft copolymer

P(VDF-*co*-CTFE)-g-PSSA graft copolymer was synthesized via a single-step ATRP reaction using CTFE unit as a macroinitiator, according to previous work [20]. Two grams of P(VDF-*co*-CTFE) were dissolved in 50 mL NMP in a round flask at 80 °C. Separately, 11 g of SSA was dissolved in 40 mL DMSO at 80 °C and was added to a P(VDF-*co*-CTFE) solution. After preparing a homogeneous solution, 0.16 g of CuCl and 0.4 mL of HMTETA were added, and the reaction flask was sealed with a rubber septum. The reaction mixture was purged with N_2 for 30 min, and the vessel was immersed in an oil bath at 90 °C. The reaction was allowed to proceed for 24 h. After dilution with DMSO, the solutions were passed through a column with activated Al_2O_3 to remove the catalyst and were then precipitated into methanol. The polymer was purified via redissolution in DMSO and reprecipitation in methanol. Finally, the P(VDF-*co*-CTFE)-g-PSSA graft polymer was dried in a vacuum oven overnight at room temperature.

Membrane preparation

An outline for the preparation of the nanocomposite membrane is shown in Scheme 1. The amount of silica in the P(VDF-*co*-CTFE)-*g*-PSSA solution was varied to obtain different MPTMS contents in the range of 0–20 wt.% in the membrane. Solutions were further stirred for 24 h at room temperature to encourage a sol–gel reaction. The mole ratio used in the sol–gel reaction was MPTMS/water/ethanol/HCl=1:4:2.34:0.08. The prepared mixture was slowly poured into a glass dish and was held in an oven at 80 °C for 24 h followed by vacuum evacuation for complete removal of the residual solvent. The dried nanocomposite membranes were oxidized via immersion in a 10 wt.% H_2O_2 solution for 1 h at 64 °C, resulting in conversion to sulfonated silica [18]. Finally, the sodium salt ($-SO_3Na$) form in PSSA was transformed to its protonated form ($-SO_3H$) through ion exchange with sulfuric acid for 24 h. The protonated P(VDF-*co*-CTFE)-*g*-PSSA/SiO_2-SO_3H nanocomposite membranes were washed with water repeatedly and dried in an oven.

Ion exchange capacity

The ion exchange capacity (IEC) values of the membranes were measured according to the classical titration method. The membranes were soaked in a 1.0-M NaCl solution for 24 h before measuring the IEC. The protons released due to the exchange reaction with Na ions were titrated against 0.01 M standardized NaOH solution using a phenolphthalein indicator. The IECs of the graft copolymer membranes were calculated using the following equation:

$$\mathrm{IEC(milli\ equivalent/gram)} = \frac{X \times N_{\mathrm{NaOH}}}{\mathrm{Weight(polymer)}}, \qquad (1)$$

where X is the volume of NaOH consumed and N_{NaOH} is the normality of NaOH. The reported IEC values were the mean of at least five measurements.

Water uptake

Water uptake was determined by weighing a vacuum-dried membrane and a membrane fully equilibrated with water. The surface of the membrane sample was wiped with an absorbent paper to remove excess water, and the sample was then weighed. The water uptake of the membranes was determined from

$$\mathrm{Water\ uptake(weight\ percent)} = \frac{W_{\mathrm{w}} - W_{\mathrm{d}}}{W_{\mathrm{d}}} \times 100, \qquad (2)$$

where W_{w} and W_{d} are the weights of wet and dried membranes, respectively. The values of the water content reported are the mean of at least five measurements.

Proton conductivity

A four-point probe method was used to measure the proton conductivities of the membranes using a ZAHNER IM-6 impedance analyzer [20–22]. The salt-form membranes

were converted into the acid form via submersion in 0.5 M H_2SO_4 solution for 16 h, followed by washing with deionized water. Before the measurement of proton conductivity, the prepared membranes were equilibrated with deionized water. Complex impedance measurements were carried out in a frequency range of 1–8 MHz at 25 °C using a ZAHNER IM-6 impedance analyzer. The impedance spectra of the membranes were used to generate Nyquist plots, and the proton conductivity was calculated from the plots. The impedance of each sample was measured five times to ensure good data reproducibility.

Characterization

FT-IR spectra of the samples were collected using an Excalibur Series FT-IR (DIGLAB Co.) instrument over the frequency range of 4,000–400 cm^{-1} using an attenuated total reflection facility. WAXS measurements were performed with a Rigaku D/max-RB apparatus (Tokyo, Japan). Data were collected from 5° to 60° at a rate of 1°/min. SAXS data were measured at the 4C1 beamline at the Pohang Light Source (PLS), Korea. The operating conditions were set to a wavelength of 1.608 Å, sample-to-detector distance of 2 m, and beam size of 1×1 mm^2. TEM images were obtained from a Philips CM30 microscope operating at 300 kV. For TEM measurements, a drop of sol–gel solution was placed directly onto a standard copper grid. The thermal properties of the membranes were determined using thermal gravimetric analysis (TGA, Mettler Toledo TGA/SDTA 851e, Columbus, OH) under a nitrogen atmosphere from room temperature to 700 °C at a rate of 20 °C/min. Tensile evaluation was performed on a universal testing machine (UTM, a LR10KPlus Series) at a speed of 5 mm/min. The reported values were the mean of five experiments. The standard deviations from the mean values of Young's modulus and tensile strength were ±5% and ±6%, respectively.

MEA fabrication

MEA were fabricated using a catalyst-coated membrane method with a well-dispersed catalyst slurry that was sprayed onto the membranes at ambient temperature. The slurry containing 0.3 g of carbon supported Pt, 1.2 g deionized water, 2.4 g Nafion® solution (5 wt.% Nafion® 1100), and 3.6 g of isopropyl alcohol were mixed for using catalyst ink. For mixing the ionomer and Pt particles, the catalyst slurries were mechanically stirred and ultrasonicated. Each step was repeated five times alternately. The catalyst inks were then sprayed on to the membranes using an airbrush gun with a catalyst loading 0.4 mg cm^{-2} at both the anode and cathode. Both of the electrodes had an active surface area of 4 cm^2. After that, the catalyst-coated membranes were dried at 100°C for 1 h to remove the residual solvent. The single fuel cell was prepared with the assembly of catalyst-coated membrane, gas diffusion media (SGL 10BC) and Teflon gasket, without hot pressing.

Results and discussion

Preparation of nanocomposite membranes

The preparation of proton-conducting nanocomposite membranes consisting of a P(VDF-*co*-CTFE)-*g*-PSSA-grafted polymer and sulfonated SiO_2 (SiO_2–SO_3H) nanoparticles via a sol–gel, and the oxidation process is illustrated in Scheme 1. The free-standing nanocomposite membranes possessed good film-forming properties with a thickness of about 50 μm and good flexibility, as shown in Fig. 1. All of the membranes were transparent or semi-transparent; transparency decreased with increasing SiO_2 content.

Figure 2a shows the FT-IR spectra of P(VDF-*co*-CTFE)-*g*-PSSA/MPTMS nanocomposite membranes with different MPTMS concentrations. The pristine P(VDF-*co*-CTFE)-*g*-PSSA graft copolymer exhibited several absorption bands at 1,174, 1,125, and 1,034 cm^{-1}, attributable to the stretching vibrations of phenyl rings substituted with sulfonate groups and sulfonate anions [20]. Upon the addition of MPTMS to the P(VDF-*co*-CTFE)-*g*-PSSA matrix, the intensity of the absorption peak at 995 cm^{-1} increased due to the symmetric stretching vibration of the Si–O–Si groups [17, 18]. Figure 2b shows the FT-IR spectra of P(VDF-*co*-CTFE)-*g*-PSSA/SiO_2-SO_3H nanocomposite membranes after oxidation of the thiol groups (−SH) of SiO_2 to the sulfonic groups (−SO_3H) using H_2O_2. After oxidation, SO_3H group peaks were observed at 1,180, 1,130, and 1,039 cm^{-1}, resulting from the S=O stretching vibrations of sulfonic acids of silica. Upon comparing P(VDF-*co*-CTFE)-*g*-PSSA graft copolymer before and after the oxidation process (Fig. 2a, b with 0 wt.%), the absorption bands at 1,174, 1,125, and 1,034 cm^{-1} were weakened, implying some degradation of PSSA by oxidation. Figure 2c shows the FT-IR spectra of P(VDF-*co*-CTFE)-*g*-PSSA/SiO_2-SO_3H nanocomposite membranes after the ion exchange of Na ions with proton ions in PSSA. The S=O stretching vibration peaks of the SO_3H group were observed at 1,161, 1,125, 1,033, and 1,006 cm^{-1}. These FT-IR results strongly support the performance of successful sol–gel reaction, oxidation, and ion exchange of the membranes.

IEC, water uptake, and conductivity

The IEC values of P(VDF-*co*-CTFE)-*g*-PSSA/SiO_2-SO_3H membranes are shown in Fig. 3. The sulfonic acid group

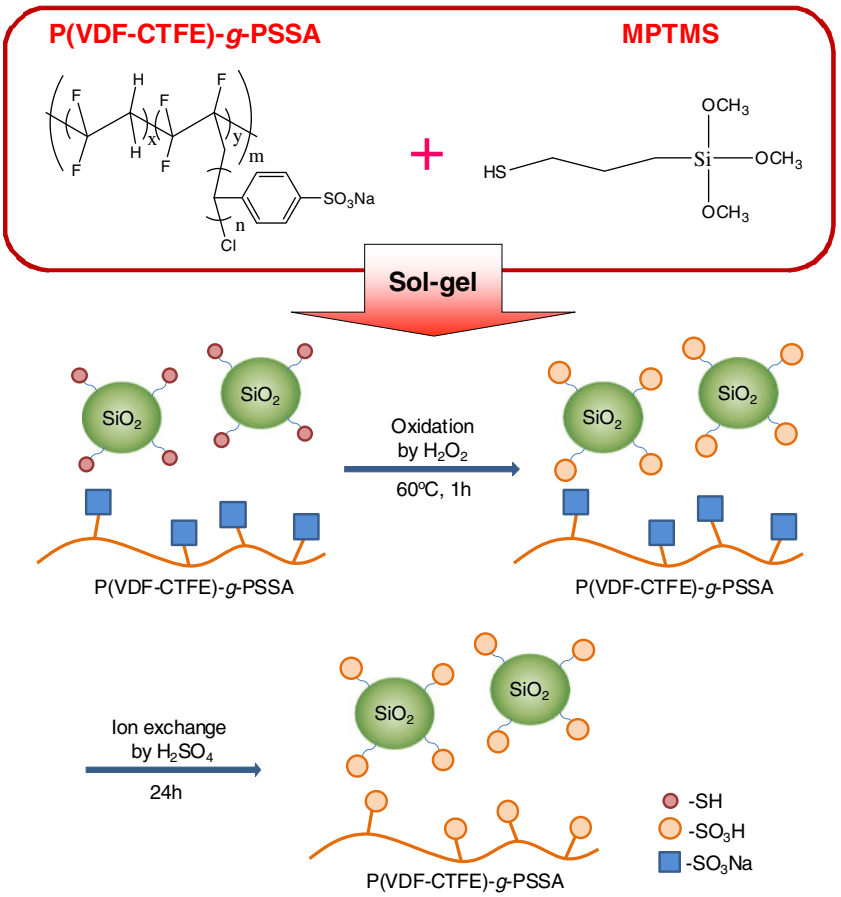

Scheme 1 Schematic illustration for the preparation of nanocomposite membranes consisting of P(VDF-*co*-CTFE)-*g*-PSSA graft copolymer and sulfonated SiO_2

has the ability to exchange ions; therefore, the quantity of sulfonic groups should be proportional to the ion exchange capability. The initial IEC value of P(VDF-*co*-CTFE)-*g*-PSSA without oxidation was 0.8 mEq/g, which was reduced to 0.45 after oxidation due to some degradation of PSSA, as confirmed by FT-IR spectroscopy. However, the IEC values of P(VDF-*co*-CTFE)-*g*-PSSA/SiO_2-SO_3H nanocomposite membranes significantly increased with MPTMS content, ranging between 0.8 and 1.0 mEq/g comparable to that of Nafion.

Figure 4 shows the water uptake value as a function of MPTMS content. Similar to the IEC graph, the initial water uptake of P(VDF-*co*-CTFE)-*g*-PSSA was reduced from 45 to 27 wt.% after oxidation process and increased with increasing MPTMS concentration, indicating that these properties are strongly related to each other. The sulfonic acid groups of silica are hydrophilic, and hence the membranes with higher MPTMS can absorb more water. When the MPTMS content was further increased, the proportion of sulfonic groups in the membranes increased. This effect was maximized at a concentration of 5 wt.% MPTMS, above which the water uptake decreased. This may be due to the fact that higher inorganic component concentration results in macroscopically phase-separated and denser structures, reducing the swelling ability of the membranes [23]. This structural change was monitored using WAXS, TEM, and SAXS analysis.

The proton conductivity behaviors of the nanocomposite membranes are presented in Fig. 5. As shown, proton conductivity increased with an increase in MPTMS content

Fig. 1 Photographs of P(VDF-*co*-CTFE)-*g*-PSSA/SiO_2-SO_3H nanocomposite membranes; MPTMS content is **a** 5 wt.%, **b** 10 wt.%, and **c** 20 wt.%

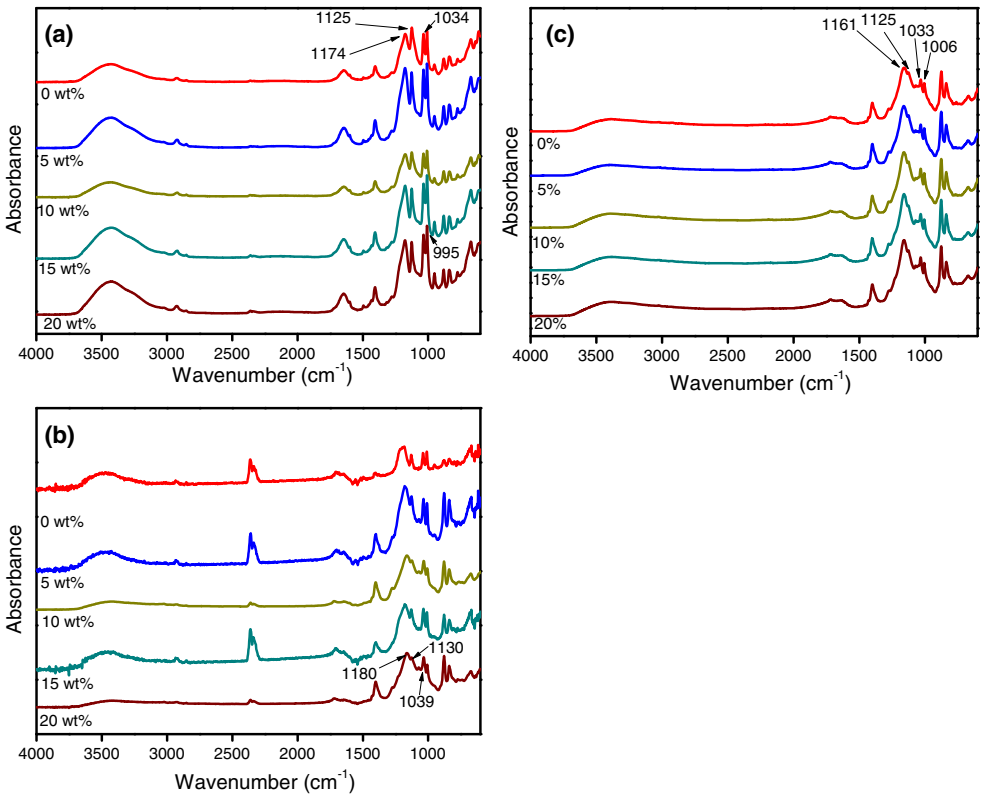

Fig. 2 FT-IR spectra of P(VDF-*co*-CTFE)-*g*-PSSA/MPTMS nanocomposite membranes with different compositions: **a** with no treatment, **b** after oxidation with H_2O_2, and **c** after ion exchange with H_2SO_4

and reached a maximum value of 0.12 S/cm at 5 wt.% MPTMS. This value was about 30% higher than that of Nafion 117 membranes at the same experimental conditions. These results demonstrate that MPTMS plays an important role in increasing proton conductivity due to the increase in the presence of sulfonic groups in the membrane. However, the proton conductivity value decreased with increasing MPTMS content above 5 wt.% due to a denser structure as well as phase separation between the graft copolymer and silica, consistent with the water uptake and IEC data. The proton conductivity of membranes increased with an increase in temperature. In particular, the conductivity at 75 °C, which is the temperature for MEA performance test, reached 0.18 S/cm for the membrane with 5 wt.% of MPTMS. It is because the elevation of temperature favors both the dynamics of proton

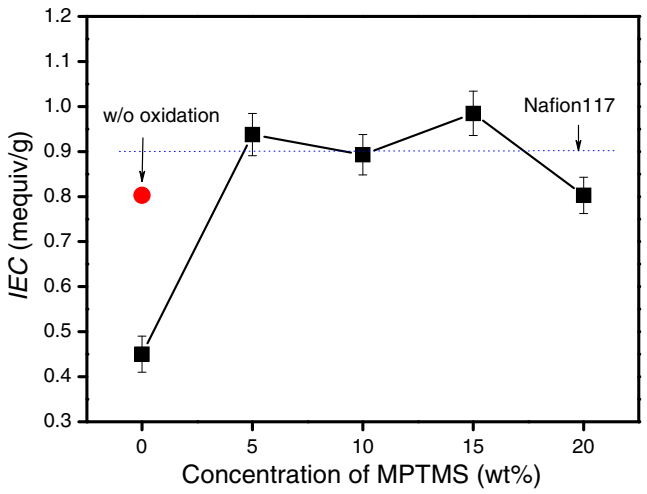

Fig. 3 IEC values of P(VDF-*co*-CTFE)-*g*-PSSA/SiO_2-SO_3H nanocomposite membranes after oxidation as a function of MPTMS concentration. The data of Nafion 117 and P(VDF-*co*-CTFE)-*g*-PSSA without oxidation are included

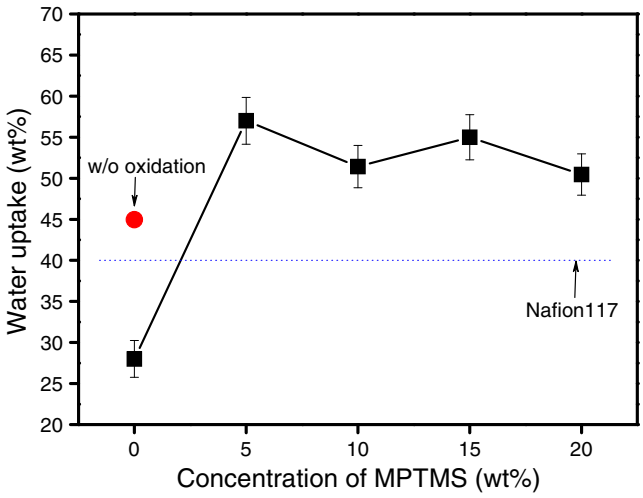

Fig. 4 Water uptake of P(VDF-*co*-CTFE)-*g*-PSSA/SiO_2-SO_3H nanocomposite membranes after oxidation as a function of MPTMS concentration. The data of Nafion 117 and P(VDF-*co*-CTFE)-*g*-PSSA without oxidation are included

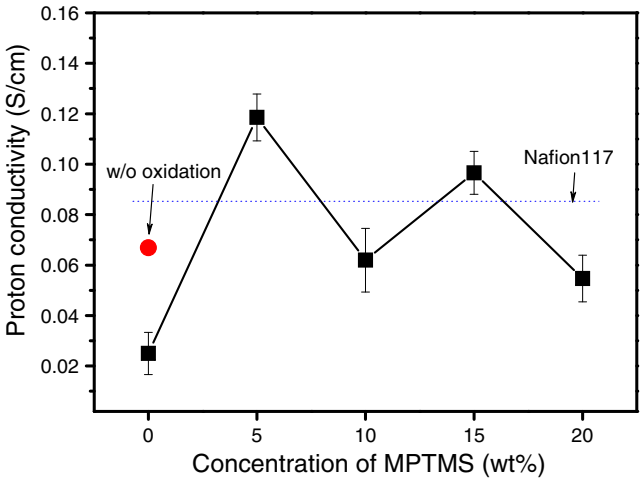

Fig. 5 Proton conductivities of P(VDF-*co*-CTFE)-*g*-PSSA/SiO_2-SO_3H nanocomposite membranes after oxidation as a function of MPTMS concentration at 25 °C. The data of Nafion 117 and P(VDF-*co*-CTFE)-*g*-PSSA without oxidation are included

transport and the structural reorganization of polymeric chains, resulting in the increased proton conductivity at high temperatures.

Membrane structure and morphology

The XRD diffraction patterns of nanocomposite membranes containing 0–20 wt.% MPTMS are presented in Fig. 6. Pristine P(VDF-*co*-CTFE)-*g*-PSSA graft copolymer exhibited broad amorphous halos centered at 18.2° and 20.2°. In general, the intensities of the peaks were reduced as the concentration of MPTMS increased, implying that silica perturbed the microstructures of the graft copolymer membranes [24]. In addition to microstructural changes, the nanostructural changes in the membranes as a result of the addition of silica were also investigated using SAXS analysis. SAXS is a well-established experimental technique to complement the structural analysis obtained from

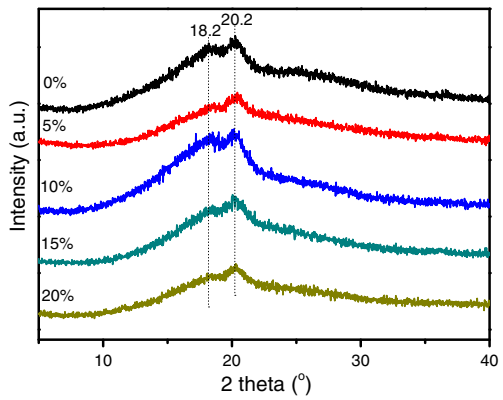

Fig. 6 WAXS patterns of P(VDF-*co*-CTFE)-*g*-PSSA/SiO_2-SO_3H nanocomposite membranes as a function of MPTMS concentration

microscopy images because it provides information over a large sample area [25, 26]. The SAXS profiles of the nanocomposite membranes with different MPTMS concentrations are plotted against the scattering vector, q, in Fig. 7a. The pristine graft copolymer exhibited a maximum peak at q=0.207 nm^{-1}, suggesting that it had a well-developed, nanophase-separated structure. Upon the addition of MPTMS, the nanocomposite membranes remained in a microphase-separated state, but their q value maxima shifted to higher values. At the same time, the peaks became broader with increasing MPTMS concentration. The domain spacing of the graft polymer was estimated from the peak maximum using the Bragg relationship. Figure 7b shows that the domain spacing of P(VDF-*co*-CTFE)-*g*-PSSA decreased from 30 to 17 nm with increasing MPTMS concentration up to 5%, above which it did not change greatly. Instead, additional domain spacing was observed near 40 nm at concentrations greater than 5 wt.% MPTMS which increased linearly with increasing MPTMS

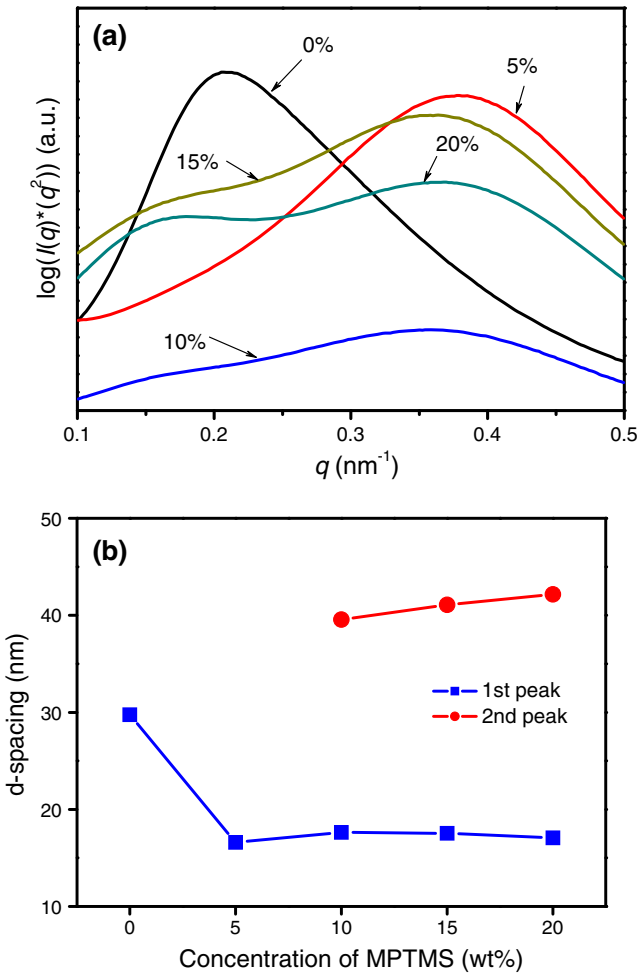

Fig. 7 **a** SAXS patterns and **b** d-spacing of P(VDF-*co*-CTFE)-*g*-PSSA/SiO_2-SO_3H nanocomposite membranes with different MPTMS contents

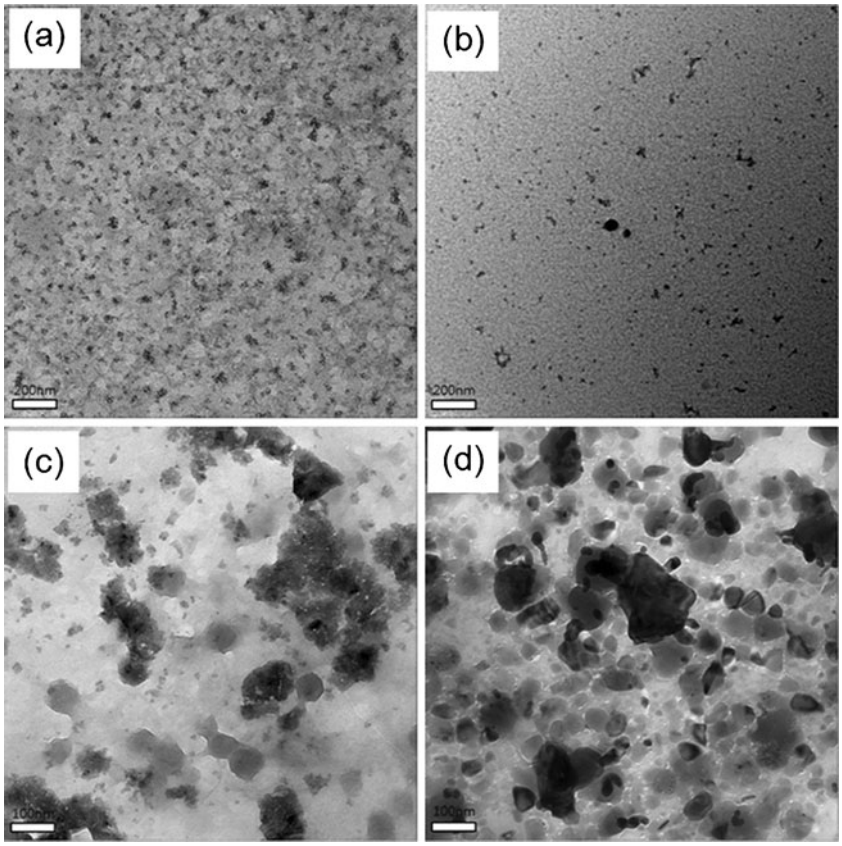

Fig. 8 TEM images of P(VDF-*co*-CTFE)-*g*-PSSA/SiO_2-SO_3H nanocomposite membranes with different MPTMS contents. **a** 0 wt.%, **b** 5 wt.%, **c** 10 wt.%, and **d** 15 wt.%

concentration. This suggests that the microphase-separated structure of the graft copolymer was maintained up to 5 wt.% MPTMS, above which the organic graft copolymer and the inorganic silica were macroscopically phase-separated due to a miscibility limit between them. These morphological properties affect the properties of P(VDF-*co*-CTFE)-*g*-PSSA/SiO_2-SO_3H membranes, in which both the water uptake and proton conductivity were the greatest at 5 wt.% of silica.

Figure 8 shows the TEM images of P(VDF-*co*-CTFE)-*g*-PSSA/SiO_2-SO_3H membranes with different concentrations of MPTMS. The pristine P(VDF-*co*-CTFE)-*g*-PSSA graft copolymer exhibited a well-developed phase-separated structure, consistent with the SAXS data of Fig. 7. The bright regions were due to the P(VDF-*co*-CTFE) main chains, whereas PSSA side chains appeared dark due to their high electron densities [20]. Upon introduction of MPTMS, additional dark regions were observed due to the formation of silica particles. The silica nanoparticles, about 5–10 nm in average size, were well distributed within the graft copolymer at 5 wt.% MPTMS. However, silica nanoparticles were more than 50 nm in size and aggregated at concentrations greater than 5 wt.% of MPTMS, which consequently enhanced the resistance to proton transfer. These TEM results are in good agreement with the SAXS data of Fig. 7.

Mechanical and thermal properties of membranes

Mechanical properties of membranes are of pivotal importance in MEA applications. The stress–strain curves of P(VDF-*co*-CTFE)-*g*-PSSA/SiO_2-SO_3H membranes are presented in Fig. 9, and the properties were summarized in Table 1. An increase in the Young's modulus of the

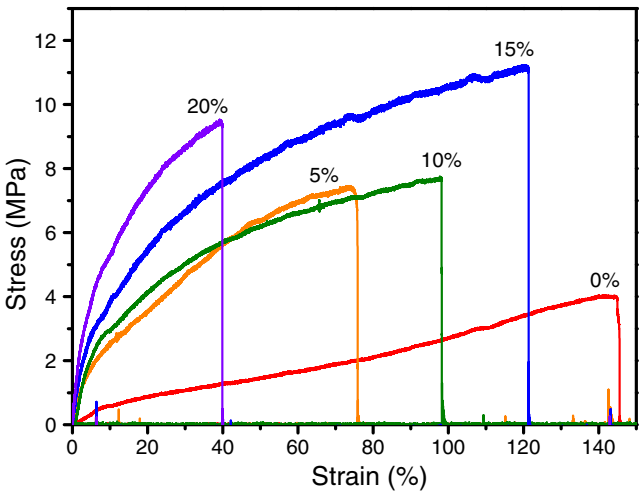

Fig. 9 Stress–strain curves of P(VDF-*co*-CTFE)-*g*-PSSA/SiO_2-SO_3H nanocomposite membranes with different MPTMS contents

Table 1 Tensile strength, elongation at break, and Young's modulus of P(VDF-*co*-CTFE)-*g*-PSSA/SiO_2-SO_3H membranes

MPTMS	Tensile strength at break (MPa)	Elongation at break (%)	Young's modulus (MPa)
0 wt.%	4.5	145	6.9
5 wt.%	7.4	74	31.9
10 wt.%	7.6	97	40.8
15 wt.%	11.2	121	60.6
20 wt.%	9.3	39	133.8
Nafion117	14.8	250	363.4

nanocomposite membrane was observed with increasing MPTMS content. However, the tensile strength and elongation at break did not continuously increase with the increasing MPTMS content. Generally, the tensile strength at break increased, whereas the elongation at break decreased with MPTMS. This is because the graft copolymer became denser due to reduced flexibility of the chains upon the introduction of silica. The mechanical properties, especially the elongation at break and Young's modulus of P(VDF-*co*-CTFE)-*g*-PSSA/SiO_2-SO_3H membranes were smaller than those of Nafion117.

Figure 10 shows TGA data of P(VDF-*co*-CTFE)-*g*-PSSA/SiO_2-SO_3H nanocomposite membranes with different concentrations of MPTMS. The first weight loss observed, which occurs at temperatures up to 100 °C, was due to dehydration. The second weight loss between 200 and 300 °C is attributed to the decomposition of the sulfonic acid group. Another weight loss in the range of 300–500 °C was due to the decomposition of the propylsulfonic acid group incorporated in the materials, which increased with increasing MPTMS from 0 to 20 wt. % [27]. The final residue above 700 °C continuously decreased with increasing MPTMS content, implying higher thermal stability of PVDF-based polymer compared to that of inorganic MPTMS. This is presumably due to some incomplete condensation of the methoxy groups of MPTMS onto the framework as the intermolecular interactions between the organic moieties increase [23, 27].

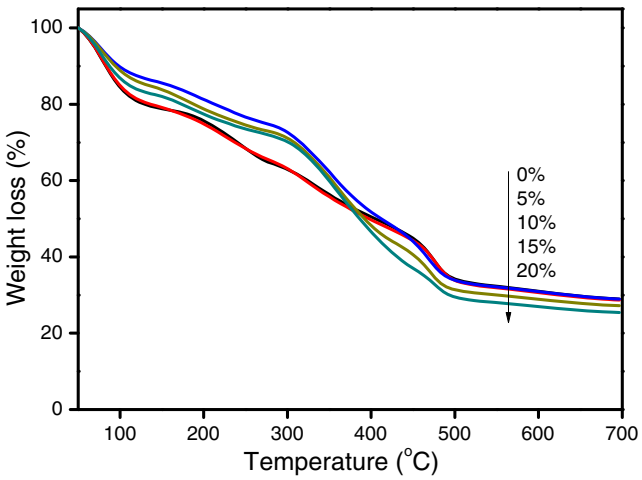

Fig. 10 TGA curves of P(VDF-*co*-CTFE)-*g*-PSSA/SiO_2-SO_3H nanocomposite membranes with different MPTMS contents

MEA performance

The single cell PEMFC performance using H_2/O_2 was tested for the P(VDF-*co*-CTFE)-*g*-PSSA/SiO_2-SO_3H nanocomposite membranes at 75 °C, and the results are presented in Fig. 11. In general, cell performance increased with increasing silica content. The maximum performance was obtained for the membrane with 5 wt.% of MPTMS, which showed 0.95 A/cm^2 of current density at 0.6 V. The power density of the H_2/O_2 fuel cells reached 1.0 W/cm^2 at 75 °C. This MEA performance is consistent with the results of proton conductivity in that the membrane with 5 wt.%

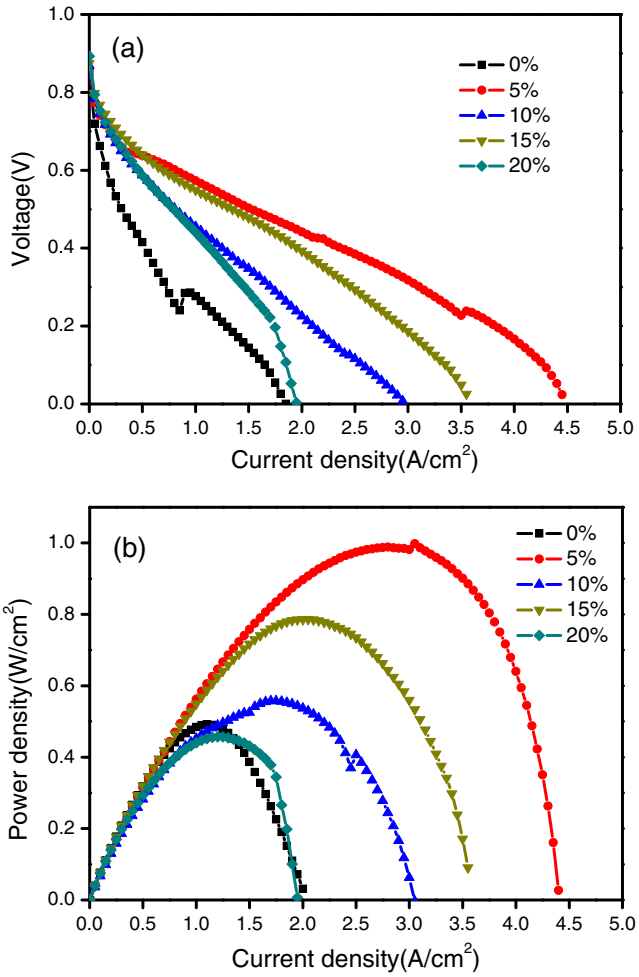

Fig. 11 **a** Current density vs. voltage curves, **b** power density vs. current density curves for P(VDF-*co*-CTFE)-*g*-PSSA/SiO_2-SO_3H nanocomposite membranes with different MPTMS contents at 75 °C

MPTMS loading showed better performance than did the other compositions. TEM and SAXS analyses revealed that the small silica nanoparticles were homogeneously distributed within the graft copolymer up to 5 wt.% of MPTMS, above which miscibility between the graft copolymer and silica decreased. As a result, MEA performance as well as membrane proton conductivity decreased above 5 wt.% MPTMS.

Conclusions

A series of proton conducting nanocomposite membranes were prepared based on P(VDF-*co*-CTFE)-*g*-PSSA graft copolymer and the sol–gel reaction of MPTMS. The resultant nanocomposite membranes were characterized using FT-IR, IEC, water uptake, proton conductivity, WAXS, SAXS, UTM, TEM, and single cell MEA performance. The silica was homogenously incorporated into the P(VDF-*co*-CTFE)-*g*-PSSA polymer matrix up to 5 wt.% MPTMS, above which macroscopic phase-separation was observed. As a result, the water uptakes and proton conductivities of membranes increased with silica content up to 5 wt.%, above which these measures decreased with increased silica. All of the membranes were in the amorphous state, were semi-transparent and thermally stable. All of the nanocomposite membranes also exhibited good mechanical properties. For example, the membrane with 5 wt.% of MPTMS exhibited a 7.4-MPa tensile strength, 74% elongation at break and a Young's modulus of 31.9 MPa, a proton conductivity of 0.12 S/cm at 25 °C and a power density of 1.0 W/cm^2 at 75 °C for H_2/O_2 fuel cells.

Acknowledgment This work was supported by the Ministry of Knowledge Economy through the Human Resources Development of the Korea Institute of Energy Technology Evaluation and Planning (KETEP) (20104010100500) and the New and Renewable Energy R&D program (2009T100100606). This work was also supported by a National Research Foundation (NRF) grant funded by the Korean government (MEST) through the Korea Center for Artificial Photosynthesis (KCAP) located in Sogang University (NRF-2009-C1AAA001-2009-0093879).

References

1. Steele BCH, Heinzel A (2001) Materials for fuel-cell technologies. Nature 414:345–352
2. Roy A, Hickner MA, Einsla B, Harrison WL, McGrath JE (2009) Synthesis and characterization of partially disulfonated hydroquinone-based poly(arylene ether sulfone)s random copolymers for application as proton exchange membranes. J Polym Sci A: Polym Chem 47:384–391
3. Kamarudin SK, Achmad F, Daud WRW (2009) Overview on the application of direct methanol fuel cell (DMFC) for portable electronic devices. Int J Hydrogen Energy 34:6902–6916
4. Esmaeilifar A, Rowshanzamir S, Eikani MH, Ghazanfari E (2010) Synthesis methods of low-Pt-loading electrocatalysts for proton exchange membrane fuel cell systems. Energy 35:3941–3957
5. Itoh T, Hirai K, Tamura M, Uno T, Kubo M, Aihara Y (2010) Synthesis and characteristics of hyperbranched polymer with phosphonic acid groups for high-temperature fuel cells. J Solid State Electrochem 14:2179–2189
6. Peighambardoust SJ, Rowshanzamir S, Amjadi M (2010) Review of the proton exchange membranes for fuel cell applications. Int J Hydrogen Energy 35:9349–9384
7. Sahu AK, Bhat SD, Pitchumani S, Sridhar P, Vimalan V, George C, Chandrakumar N, Shukla AK (2009) Novel organic–inorganic composite polymer-electrolyte membranes for DMFCs. J Membr Sci 345:305–314
8. Verma A, Scott K (2010) Development of high-temperature PEMFC based on heteropolyacids and polybenzimidazole. J Solid State Electrochem 14:213–219
9. Matos BR, Santiago EI, Rey JFQ, Ferlauto AS, Traversa E, Linardi M, Fonseca FC (2011) Nafion-based composite electrolytes for proton exchange membrane fuel cells operating above 120 °C with titania nanoparticles and nanotubes as fillers. J Power Sources 196:1061–1068
10. Umeda J, Suzuki M, Kato M, Moriya M, Sakamoto W, Yogo T (2010) Proton conductive inorganic–organic hybrid membranes functionalized with phosphonic acid for polymer electrolyte fuel cell. J Power Sources 195:5882–5888
11. Xiang Y, Yang M, Guo Z, Cui Z (2009) Proton conductive inorganic–organic hybrid membranes functionalized with phosphonic acid for polymer electrolyte fuel cell. J Membr Sci 337:318–323
12. Amjadi M, Rowshanzamir S, Peighambardoust SJ, Hosseini MG, Eikani MH (2010) Investigation of physical properties and cell performance of Nafion/TiO_2 nanocomposite membranes for high temperature PEM fuel cells. Int J Hydrogen Energy 35:9252–9260
13. Sahu AK, Selvarani G, Bhat SD, Pitchumani S, Sridhar P, Shukla AK, Narayanan N, Banerjee A, Chandrakumar N (2008) Effect of varying poly(styrene sulfonic acid) content in poly(vinyl alcohol)–poly(styrene sulfonic acid) blend membrane and its ramification in hydrogen–oxygen polymer electrolyte fuel cells. J Membr Sci 319:298–305
14. Ahmad H, Kamarudin SK, Hasran UA, Daud WRW (2010) Overview of hybrid membranes for direct-methanol fuel-cell applications. Int J Hydrogen Energy 35:2160–2175
15. Santiago EI, Isidoro RA, Dresch MA, Matos BR, Linardi M, Fonseca FC (2009) Nafion–TiO_2 hybrid electrolytes for stable operation of PEM fuel cells at high temperature. Electochim Acta 54:4111–4117
16. Niepcerona F, Lafittea B, Galianoa H, Bigarrea J, Nicol E, Tassin JF (2009) Composite fuel cell membranes based on an inert polymer matrix and proton-conducting hybrid silica particles. J Membr Sci 338:100–110
17. Guo R, Ma X, Hu C, Jiang Z (2007) Novel PVA–silica nanocomposite membrane for pervaporative dehydration of ethylene glycol aqueous solution. Polymer 48:2939–2945
18. Yen CY, Lee CH, Lin YF, Lin HL, Hsiao YH, Liao SH, Chuang CY, Ma CCM (2007) Novel PVA–silica nanocomposite membrane for pervaporative dehydration of ethylene glycol aqueous solution. J Power Sources 173:36–44
19. Kim YK, Choi YG, Kim HK, Lee JS (2010) New sulfonic acid moiety grafted on montmorillonite as filler of organic–inorganic composite membrane for non-humidified proton-exchange membrane fuel cells. J Power Sources 195:4653–4659
20. Kim YW, Choi JK, Park JT, Kim JH (2008) Proton conducting poly(vinylidene fluoride-co-chlorotrifluoroethylene) graft copolymer electrolyte membranes. J Membr Sci 313:315–322

21. Kim YW, Park JT, Koh JH, Roh DK, Kim JH (2008) Anhydrous proton conducting membranes based on cross-linked graft copolymer electrolytes. J Membr Sci 325:319–325
22. Roh DK, Ahn SH, Seo JA, Shul YG, Kim JH (2010) Synthesis and characterization of grafted/crosslinked proton conducting membranes based on amphiphilic PVDF copolymer. J Polym Sci B: Polym Phys 48:1110–1117
23. Tsai JC, Kuo JF, Chen CY (2007) New sulfonic acid moiety grafted on montmorillonite as filler of organic–inorganic composite membrane for non-humidified proton-exchange membrane fuel cells. J Power Sources 174:103–113
24. Kalappa P, Lee JH (2007) Proton conducting membranes based on sulfonated poly(ether ether ketone)/TiO_2 nanocomposites for a direct methanol fuel cell. Polym Int 56:371–375
25. Olivetti EA, Kim JH, Sadoway DR, Asatekin A, Mayes AM (2006) Sol−gel synthesis of vanadium oxide within a block copolymer matrix. Chem Mater 18:2828–2833
26. Kim YW, Lee DK, Lee KJ, Min BR, Kim JH (2007) In situ formation of silver nanoparticles within an amphiphilic graft copolymer film. J Polym Sci B: Polym Phys 45:1283–1290
27. Li YS, Church JS, Woodhead AL, Moussa F (2010) Preparation and characterization of silica coated iron oxide magnetic nano-particles. Spectrochimica Acta A 76:484–489